Proceedings of the 18th International Symposium on the Packaging and Transportation of Radioactive Materials
PATRAM 2016
September 18-23, 2016, Kobe, Japan

Paper No.2051

Impact of Reactor Operating Parameters on Cask Reactivity in BWR Burnup Credit

Germina Ilas, Ben Betzler, and Brian Ade[1]
Oak Ridge National Laboratory
1 Bethel Valley Road, Oak Ridge, TN 37831, USA
ilasg@ornl.gov

Abstract

This paper discusses the effect of reactor operating parameters used in fuel depletion calculations on spent fuel cask reactivity, with relevance for boiling-water reactor (BWR) burnup credit (BUC) applications. Assessments that used generic BWR fuel assembly and spent fuel cask configurations are presented. The considered operating parameters, which were independently varied in the depletion simulations for the assembly, included fuel temperature, bypass water density, specific power, and operating history. Different operating history scenarios were considered for the assembly depletion to determine the effect of relative power distribution during the irradiation cycles, as well as the downtime between cycles. Depletion, decay, and criticality simulations were performed using computer codes and associated nuclear data within the SCALE code system. Results quantifying the dependence of cask reactivity on the assembly depletion parameters are presented herein.

Introduction

Review and prioritization of technical issues related to burnup credit (BUC) for boiling-water reactor (BWR) spent fuel have previously been performed [1] to identify phenomena and parameters important to BWR BUC methodology and provide recommendations for further BWR BUC research. The three research objectives categorized as high priorities are identification and use of axial burnup profiles, treatment of axial moderator density profile, and treatment of control blade usage during depletion. These three research objectives are the subjects of recently documented investigations [2,3]. Another priority recommendation [1] for BWR BUC, categorized as a medium impact priority, included investigating additional reactor operating parameters in fuel depletion calculations, with fuel temperature, specific power, and bypass water density listed as candidates for future studies. These three medium impact parameters are considered herein, along with operating history.

This study examined the effects of reactor operating parameters used in BWR assembly depletion calculations on spent fuel cask reactivity. The fuel temperature, bypass water density, and specific power were independently varied in the assembly depletion simulations. Different operating history scenarios were considered to determine the effect of relative power changes during irradiation cycles and downtime between irradiation cycles. The assessments used the GE14 10 × 10 fuel assembly model [4] and the GBC-68 cask model [5] that have been used as reference configurations in previous studies [2–4]. The depletion, decay, and criticality simulations were performed using computer codes and associated nuclear data within the SCALE code system [6].

Computational Models

Assembly Depletion Model

The GE14 assembly under consideration contains full- and part-length fuel rods. The axial variation in geometry and operating conditions was simulated by dividing the assembly into 25 axial zones, or nodes. These axial zones considered two types of lattices: a dominant (*DOM* or *full*) lattice and a vanished (*VAN*) lattice. The geometry model for the DOM lattice is illustrated in Figure 1; it contains two large central water rods, 77 UO_2 fuel rods, and 15 gadolinium-bearing UO_2 rods. Enrichment zoning was simplified in the analysis by modeling a uniform enrichment of 4.5 wt % ^{235}U in all fuel rods. Control blades were not included in the model.

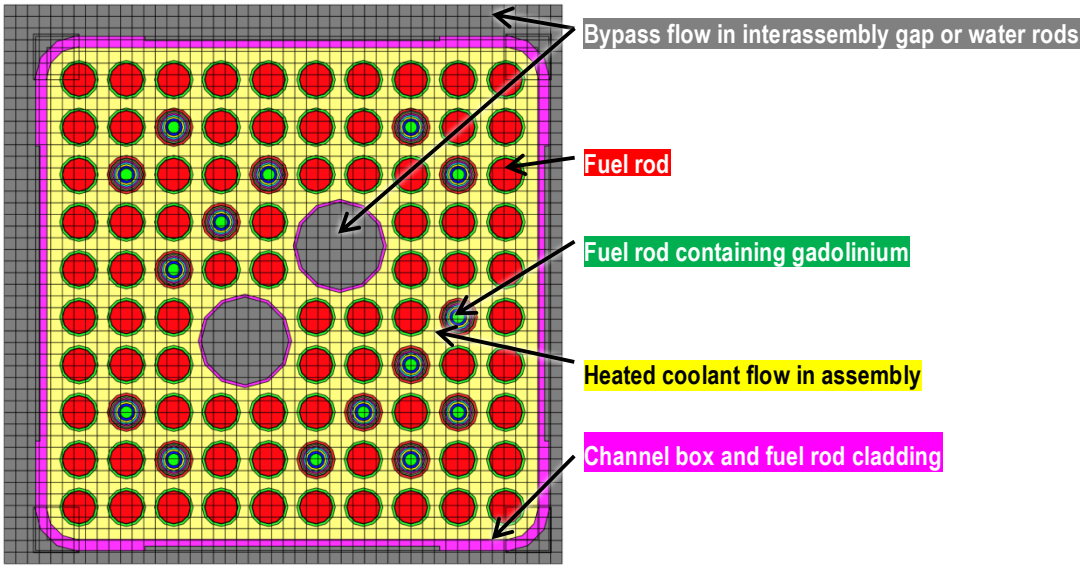

Figure 1 Assembly model (DOM lattice)

The assembly average burnup was 45.2 GWd/MTU, as used in previous studies for control blade and axial moderator profile effects [2,3]. Assembly depletion was simulated for three consecutive cycles with no downtime between the cycles for all depletion simulations described in this paper, except for the operating history scenarios. The same axial burnup profile and coolant density profile were used for all three cycles, as illustrated in Figure 2 (node 1 at top of assembly). These profiles are the same

as those used in previous control blade studies [2,3]. The VAN zones are 1-13 and the DOM zones are 14-25.

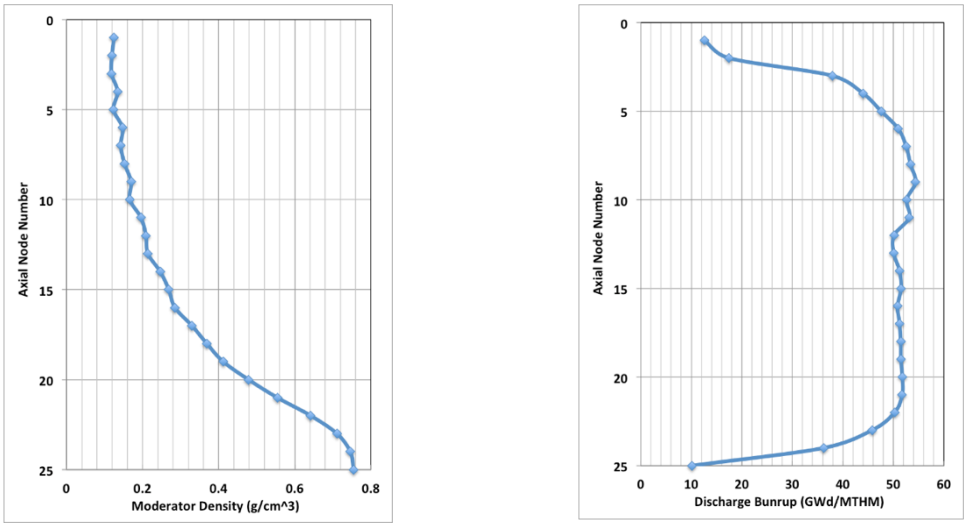

(a) Axial moderator density profile (b) Axial burnup profile

Figure 2 Axial moderator density profile and axial burnup profile

Cask Criticality Model

The GBC-68 cask criticality model is described in detail in previous reports [3–4]. This is a three-dimensional (3D) generic BUC cask [5] with explicit representation of fuel rods, including full- and part-length rods. All fuel assemblies in the cask were assumed to have the same geometry and same depleted fuel isotopic composition. The model contained 25 axial nodes (node 1 at top) in the active region of fuel rods, all of equal length. These axial nodes were consistent with the nodes used in the fuel assembly depletion model. Two sets of isotopes [7] were used for the spent fuel isotopic composition in the cask model: (1) major actinides (actinide only [AO] set) and (2) major and minor actinides plus major fission products (actinide and fission product [AFP] set); both isotope sets included ^{16}O. A radial view of the half-cask model illustrating the cask body, basket, and fuel assemblies is shown in Figure 3.

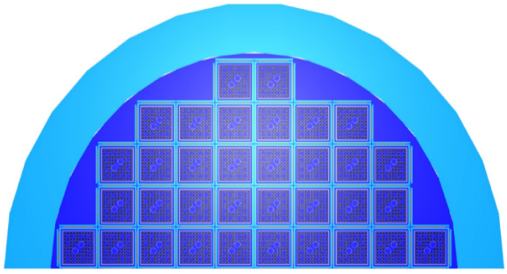

Figure 3 Radial view of the GBC-68 cask model in the VAN lattice

Computational Approach

The computational procedure to simulate the fuel assembly irradiation and the spent fuel cask reactivity includes the following main steps:

1. Depletion simulation to determine the isotopic composition of each axial zone of the irradiated fuel assembly at discharge from the reactor.
2. Decay simulation of the discharged assembly's isotopic composition to determine the nuclides present at five years' cooling time after discharge from the reactor.
3. Criticality calculation for the GBC-68 cask to determine the effective multiplication constant (k_{eff}) using the isotopic composition of the spent fuel obtained in step 2.

The assembly depletion was simulated using the TRITON t-depl sequence [8]. The assembly design and operating data used in the depletion simulations were based on a single cycle of BWR core-follow data [4]. Two-dimensional (2D) depletion simulations were performed for each of the axial slices (nodes) defined in the core-follow data (25 nodes in total). The 238-group ENDF/B-VII.0 neutron cross section library was used in the NEWT deterministic neutron transport solution in TRITON. Decay simulation of the discharged assembly's isotopic composition was performed using the ORIGEN depletion and decay code [9] in SCALE. The decay library used with ORIGEN is based on ENDF/B-VII.1 data [10]. All cask criticality calculations used the Monte Carlo neutron transport code KENO V.a [11] with a 238-group ENDF/B-VII.0 neutron cross section library. The assembly depletion calculations were performed using a pre-release version of SCALE 6.2 and the cask criticality calculations used SCALE 6.1.

Operating Parameters

The parameters that were varied in the assembly depletion model are fuel temperature, bypass water density, specific power, and operating history. All other data in this model were fixed. The considered parameters were independently varied one at a time, and no correlations between parameters were considered in this phase of the study. The values used for each parameter sensitivity study are described below.

Fuel Temperature

Increased fuel temperature in BWR depletion calculations has been shown [1,12] to lead to an increase in isotopic contents of actinides important to BUC (^{239}Pu, in particular) and consequently to an increase in cask reactivity. This effect is primarily due to increased neutron capture due to Doppler broadening of ^{238}U resonance cross sections.

Nine values were used for the fuel temperature sensitivity, covering a range from 596.1 K to 1296.1 K, in 100 K increments. The 796.1 K temperature was the reference value, representing the core- and cycle-averaged temperature over all 624 fuel assemblies in the available BWR core-follow data. The maximum temperature in the core-follow data was less than 1100 K at any time during the

cycle. To cover higher temperatures that may occur during operation [13], and for consistency with data used previously in similar BWR studies [1,12], the range was extended to ~1300 K. The depletion analyses used the same temperature in all fuel rods, with no axial or radial variation considered at this time.

Bypass Water Density

The nominal value [4] of the bypass water density was 0.73549 g/cm^3. The bypass water region corresponds to the subcooled water circulated outside the assembly channel and within the two large water rods in the assembly. This bypass water is shown with the same gray color in the illustration of the assembly configuration (see Figure 1). No axial variation was considered for the bypass water density in this study. The bypass water density is expected to be relatively invariant during steady state reactor operation. To quantify the impact resulting from density changes during operation, the sensitivity study discussed here considered 11 values that cover a range from 90% of nominal to nominal (0.73549 g/cm^3) in 1% increments. Decrease in bypass water density is expected to cause hardening of the neutron spectrum and consequently an increase in plutonium production, as well as an impact on the production of other actinides and fission products sensitive to changes in the neutron spectrum. The magnitude of this effect depends on the magnitude of the change in water density.

Specific Power

The assembly depletion simulations accounted for the axial variation of the assembly burnup, which is illustrated in Figure 2(b). The axial specific power profile and the axial burnup profile were described by the same shape (the axial distribution is the same) at discharge. The same relative power distribution was used in the three considered cases: (1) nominal, (2) 90% of nominal, and (3) 110% of nominal. The same number of depletion steps was used in each of the three cases. Because the assembly burnup at discharge was the same in these three cases, the change in specific power required a change in the total irradiation time to conserve the burnup. The irradiation time for each of the three cases was derived from this equation:

$$p_0 t_0 = k p_0 t_1 \Rightarrow t_1 = \frac{t_0}{k},$$

where p_0 and t_0 are the specific power and irradiation time for the nominal case, k is the specific power multiplier (0.9 or 1.1) for the perturbed case, and t_1 is the irradiation time for the perturbed case.

Operating History

The term *operating history* as used in this study refers to cycle length, downtime between cycles, and power level during each cycle [1]. Ten operating history scenarios investigated in this study (see

Table 1) were used to assess the effect of the power level and downtime for a given assembly burnup at discharge. Nominal conditions were used for all assembly modeling parameters for the ten operating histories under consideration. Only the power level per irradiation cycle (and equivalently burnup) and the decay time between irradiation cycles were varied. The cycle length was not changed. The OH-10 operating scenario was derived from available core-follow data.

Table 1 Operating history scenarios

History	Cycle 1		Cycle 2		Cycle 3
	% Power	Downtime (d)	% Power	Downtime (d)	% Power
OH-1	100	0	100	0	100
OH-2	100	30	100	30	100
OH-3	100	30	100	720	100
OH-4	120	30	100	30	80
OH-5	120	30	120	30	60
OH-6	100	30	120	30	80
OH-7	80	30	100	30	120
OH-8	120	30	120	720	60
OH-9	80	30	100	720	120
OH-10	136.15	30	116.53	30	47.33

Histories OH-1 through OH-3 were used to assess the impact of downtimes between cycles. Specific power was the same in each of the three cycles for these histories. History OH-1 represented continuous operation at full power with no downtime and was used as a baseline for comparison in this section. History OH-1 was used for all other sensitivity studies described in this paper (i.e., fuel temperature, bypass water density, specific power). History OH-2, with typical 30-day downtimes, assessed the effect of using typical downtime versus excluding any downtime between cycles. History OH-3 assessed the impact of extended downtime (720-days in this case) preceding the last irradiation cycle before discharge. For example, this type of scenario applies when an assembly is moved to a storage pool after two irradiation cycles, stored in the pool for approximately two years, and then irradiated for a third cycle before being permanently discharged.

Histories OH-4 through OH-7 were used to assess the effect of power variation between the three cycles when all other parameters are the same. Histories OH-4, OH-5, and OH-6 (highest power in first or second cycle, lowest power in third cycle) are considered representative of typical operation for most assemblies, whereas OH-7 (highest power in third cycle) would be atypical. Scenarios with the highest power in the second cycle would be possible for a fuel assembly with high initial gadolinium poison loadings that are depleted during the first cycle.

Histories OH-8 and OH-9 were used to assess the effect of extended downtime prior to the last irradiation cycle for a typical and an atypical power history. Except for the 720-day downtime before the third irradiation cycle, OH-8 and OH-9 were similar to OH-5 and OH-7, respectively. History OH-10 was similar to OH-4 (highest power in first cycle, lowest power in third cycle), but the power in the first two cycles was greater, while the power in the third cycle was significantly smaller.

Results

Fuel Temperature

Variation of the calculated cask k_{eff} as a function of the fuel temperature used in the assembly depletion simulation is illustrated in Figure 4. The calculated cask k_{eff} and the k_{eff} differences relative to the nominal case are shown in Table 2. The effect of fuel temperature on cask reactivity was clearly linear over the considered temperature range: reactivity increased with increasing temperature, consistent with findings from other studies [1,12]. The k_{eff} results listed in Table 2 are consistent with the expected physics behavior (e.g., resonance Doppler broadening increases with increasing temperature) and are driven by the change in isotopic composition of spent fuel as a function of temperature during depletion. As expected, the increase in cask k_{eff} with increasing temperature is mainly due to actinides (major contributors ^{235}U, ^{239}Pu, ^{241}Pu), as indicated by the small difference between cask k_{eff} calculated with the AO and AFP isotope sets for the same temperature. The magnitude of the cask reactivity increase was ~1.1 pcm/K for the AO set and ~1.0 pcm/K for the AFP set, based on the linear fit shown in Figure 4. The node average ^{239}Pu atomic density increased approximately 6% to 10%, depending on the axial node burnup, when the temperature was increased from 596 K to 1296 K.

Table 2 Cask reactivity as function of fuel temperature

Temp. (K)	AO		AFP		AO		AFP	
	k_{eff}	1σ[a]	k_{eff}	1σ	Δk_{eff}[b] (pcm[c])	1σ (pcm)	Δk_{eff} (pcm)	1σ (pcm)
596	0.82925	0.00010	0.72957	0.00010	-258	14	-231	14
696	0.83051	0.00010	0.73056	0.00010	-132	14	-133	14
796	0.83183	0.00010	0.73189	0.00010	0		0	
896	0.83268	0.00010	0.73247	0.00010	85	14	59	14
996	0.83389	0.00010	0.73343	0.00010	206	14	154	14
1096	0.83500	0.00010	0.73452	0.00010	317	14	263	14
1196	0.83577	0.00010	0.73536	0.00010	393	14	347	14
1296	0.83708	0.00010	0.73651	0.00010	525	14	462	14

[a] Standard deviation in k_{eff} as reported in the KENO output file; [b] k_{eff} difference relative to the 796K nominal case; [c] 1pcm = 0.00001

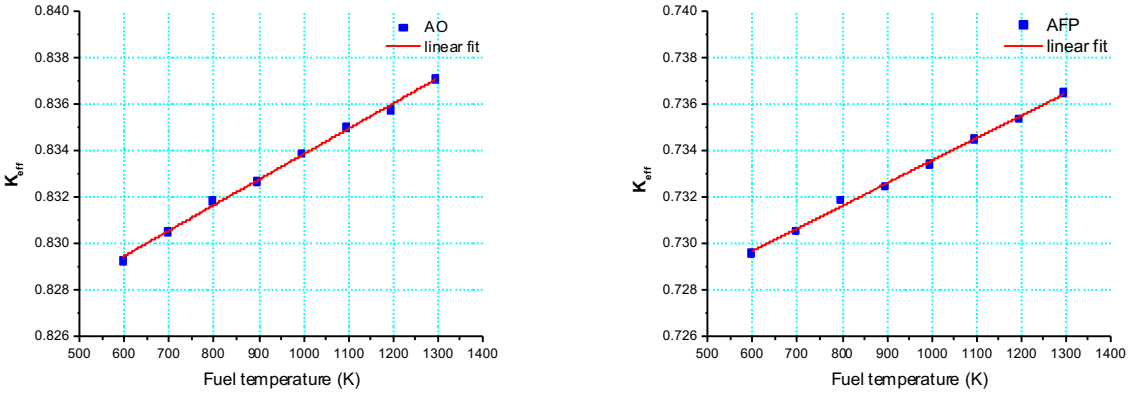

Figure 4 Effect of fuel temperature on cask k_{eff} (AO and AFP isotope sets)

Bypass Water Density

The variation of the calculated cask k_{eff} as a function of reduction in the bypass water density during the assembly depletion simulation is presented in Table 3 and illustrated in Figure 5. For the AO set, k_{eff} varied quasi-linearly over the considered range of density reduction, while for the AFP set, it varied according to a second-order polynomial. Water density reduction in the large water rods at the center of the assembly and outside the assembly channel impacts the neutron moderation in all nodes, with the actual impacts depending on the particular node environment and parameters (coolant density, burnup).

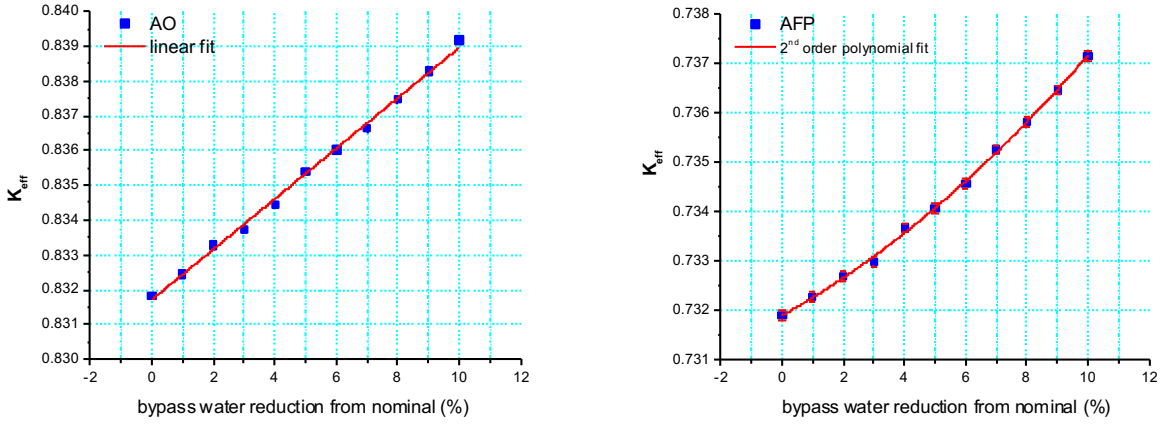

Figure 5 Effect of bypass water density on cask k_{eff} (AO and AFP isotope sets)

A 10% reduction in the bypass water density relative to its nominal value led to an increase of the assembly average ^{239}Pu content of ~7% and consequently a significant increase in cask reactivity for the studied case. The bypass water density variation during typical operation is expected to be less than 3% with respect to the nominal value, in which case the change in cask reactivity is small: less than 0.23% for the AO set and less than 0.15% for the AFP set. Even for an unlikely reduction in

bypass water density of 10%, the impact on cask reactivity (less than 0.9%) was significantly smaller than the effects of coolant density, axial burnup profile, or control blade usage [2,3]. Based on the results of this study, irrespective of the isotope set used in criticality calculations, the effect was clearly less than 0.1% Δk_{eff} for every 1% reduction in bypass water density.

Table 3 Cask reactivity as function of bypass water density reduction

Density reduction (%)	AO		AFP		AO			AFP	
	k_{eff}	1σ[a]	k_{eff}	1σ	Δk_{eff}[b] (pcm[c])	1σ (pcm)		Δk_{eff} (pcm)	1σ (pcm)
10	0.83916	0.00010	0.73716	0.00010	733	14		527	13
9	0.83828	0.00010	0.73647	0.00010	644	14		458	14
8	0.83746	0.00010	0.73581	0.00010	562	14		392	14
7	0.83662	0.00010	0.73526	0.00010	479	13		337	14
6	0.83602	0.00010	0.73456	0.00010	419	14		267	14
5	0.83539	0.00010	0.73406	0.00010	356	14		217	14
4	0.83445	0.00010	0.73367	0.00010	262	14		178	14
3	0.83374	0.00010	0.73297	0.00010	191	14		108	14
2	0.83328	0.00010	0.73269	0.00010	145	14		79	14
1	0.83245	0.00010	0.73228	0.00010	62	14		39	14
0	0.83183	0.00010	0.73189	0.00010	0	14		0	14

[a] Standard deviation in k_{eff} as reported in the KENO output file; [b] k_{eff} difference relative to nominal case; [c] 1pcm = 0.00001

Specific Power

The impact of specific power variations on cask reactivity is summarized in Table 4. The effect was extremely small for the considered magnitude of the specific power variation and not significantly higher than the statistical uncertainty in the calculated cask k_{eff}.

Table 4 Cask k_{eff} as function of change in specific power

Specific power change	AO		AFP		AO		AFP	
	k_{eff}	1σ[a]	k_{eff}	1σ	Δk_{eff}[b] (pcm[c])	1σ (pcm)	Δk_{eff} (pcm)	1σ (pcm)
+10%	0.832044	0.000099	0.731798	0.000099	21	14	-9	14
0%	0.831833	0.000099	0.731891	0.000099	0		0	
-10%	0.831538	0.000099	0.731859	0.000099	-30	14	-3	14

[a] Standard deviation in k_{eff} as reported in the KENO output file; [b] k_{eff} difference relative to 0% nominal case; [c] 1pcm = 0.00001.

Operating History

The variation of the cask k_{eff} for the considered operating histories is presented in Table 5 and illustrated in Figure 6. Figure 7 shows the impact in k_{eff} for each of the considered histories relative to history OH-1. In general, the trends of these results are similar to those identified in previous studies [12].

Table 5 Cask reactivity as function of operating history

Operating history	AO		AFP		AO		AFP	
	k_{eff}	1σ[a]	k_{eff}	1σ	Δk_{eff}[b] (pcm[c])	1σ (pcm)	Δk_{eff} (pcm)	1σ (pcm)
OH-1	0.83183	0.00010	0.73189	0.00010	0		0	
OH-2	0.83178	0.00010	0.73185	0.00010	-5	14	-4	14
OH-3	0.83116	0.00010	0.73112	0.00010	-68	14	-77	14
OH-4	0.83132	0.00010	0.73187	0.00010	-51	14	-2	14
OH-5	0.83126	0.00010	0.73192	0.00010	-57	13	3	14
OH-6	0.83162	0.00010	0.73163	0.00010	-22	14	-26	14
OH-7	0.83211	0.00010	0.73190	0.00010	28	14	1	14
OH-8	0.82996	0.00010	0.73077	0.00010	-187	14	-112	14
OH-9	0.83157	0.00010	0.73128	0.00010	-26	14	-61	14
OH-10	0.83093	0.00010	0.73166	0.00010	-90	14	-23	14

[a] Standard deviation in k_{eff} as reported in the KENO output file; [b] k_{eff} difference relative to OH-1; [c] 1pcm = 0.00001.

History OH-1 (continuous operation) resulted in the highest k_{eff}, within statistics. Irrespective of the isotope set (AO or AFP), the cask k_{eff} differences between OH-1 and other histories were either negative or statistically negligible (within two standard deviations). The only case in which the difference was not negative (although the k_{eff} values are within two standard deviations) occurred for history OH-7. Results for histories OH-1 and OH-2 are statistically equivalent, confirming that neglecting typical downtimes in depletion simulations does not impact cask reactivity.

Extended downtime later in an assembly's irradiation history led to lower cask k_{eff} for both AO and AFP isotope sets. This effect is mainly due to the decay of ^{241}Pu ($T_{1/2}$ = 14.4 yr), an actinide with significant effect on cask reactivity. The magnitude of the reactivity for the AO set was statistically similar (within 2σ) to that for the AFP isotope set. For example, for uniform power operation, an extended downtime before the last irradiation cycle (OH-3 vs. OH-1) led to a cask k_{eff} decrease by 68 pcm (1σ=14 pcm) for the AO set and 77 pcm (1σ=14 pcm) for the AFP set. These extended downtimes therefore do not require explicit modeling for conservative estimates of cask reactivity.

The effect of extended downtime before the last irradiation cycle showed the same decreasing trend

irrespective of the power level history during assembly's irradiation. Moreover, the magnitude of the decrease was similar for the AO and AFP sets given the same power history. See for example the values for OH-3 corresponding to the two isotope sets. Additionally, the magnitude varied with the power history. Operating histories OH-5 and OH-8 have the same power history (120% for the first two cycles and 60% for the last cycle), but their downtimes are much different before the last cycle.

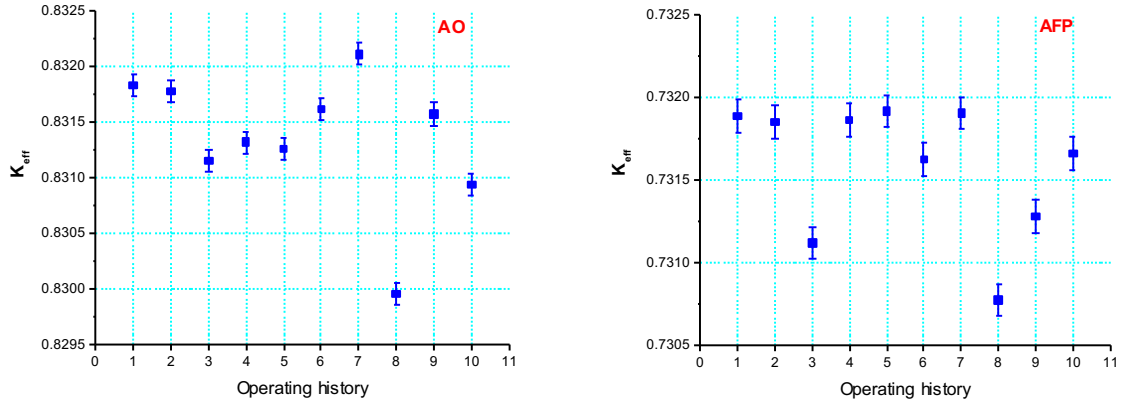

Figure 6 Effect of operating history on cask k_{eff}

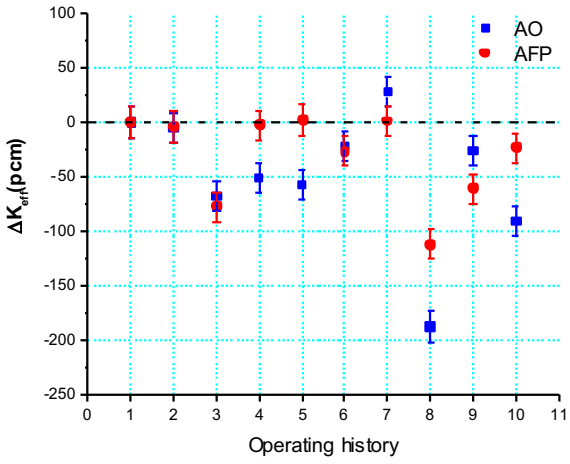

Figure 7 Effect of operating history on cask reactivity

The decrease in k_{eff} due to extended downtime before the last cycle (OH-8 vs. OH-5) for the AO and AFP sets was 130 pcm and 115 pcm, respectively. However, the magnitude of the decrease was larger in this case than for the uniform power operation (OH-3 vs. OH-1) because more plutonium was produced during the first two cycles (higher burnup at the end of the first two cycles). Another example illustrating the effect of the downtime was observed for operating histories OH-7 and OH-9, both of which have the same power history but different downtimes before the last cycle. The reactivity changes in this case (OH-9 vs. OH-7) were similar for the AO and AFP isotope sets: 54 pcm and 63 pcm decrease, respectively. The magnitude of the decrease was less than that

observed for uniform power operation (OH-3 vs OH-1), indicating once again that the magnitude of the effect depends on the power history.

Operating histories OH-4 through OH-7 illustrate the effect of the power level variation during irradiation. They all have the same downtime, but they have different, non-uniform power levels. The results indicate that the effect for the AFP isotope set was statistically negligible (within 2σ) for all operating histories in this set compared to the reference history OH-1. However, if only the AO isotope set were considered, there was a small but clear effect of the power level in the last two cycles—especially in the last cycle. For the AO isotope set, the k_{eff} value for history OH-7 was 28 pcm higher than for OH-1; however, the two k_{eff} values were within 2σ (1σ = 14 pcm).

The magnitude of the reactivity effects for the AO and AFP sets for history OH-7 were statistically the same (within 2σ). This is thought to be due to the interplay between the production and decay of those actinides and fission products with high impact on cask reactivity. This would include ^{155}Eu, which decays with a half-time of 4.75 years to ^{155}Gd, a very strong neutron absorber. In particular, for history OH-7, the ^{155}Gd assembly average atomic density for history OH-7 at 5 years' cooling was ~2% higher than the corresponding value for history OH-4.

Operating histories OH-8 and OH-9 were intended to illustrate the combined effect of the power level in the last cycle and the downtime preceding the last cycle. As seen, the combination of lower power levels during the last cycle and extended downtime preceding this cycle led to the lowest cask k_{eff} values, as also observed in other studies [12].

Operating history OH-10 showed a decrease in reactivity relative to OH-1 for both isotope sets. For the AO set, the reactivity decrease was 90 pcm. For the AFP set, the decrease was smaller, at 23 pcm. For this isotope set, the cask k_{eff} values for OH-1 and OH-10 were within 2σ (1σ = 14 pcm).

The results obtained for the ten considered operating histories indicated that the use of uniform power levels and no downtime between cycles results in the highest cask reactivity.

Conclusions

The sensitivity studies described herein evaluated the impact of selected reactor operating parameters used in depletion simulations on cask reactivity: fuel temperature, bypass water density, specific power, and operating history. These studies continue and complement previous efforts [2,3] that focused on assessing impacts of axial moderator density distributions, axial burnup distributions, and control blade exposure. The sensitivity studies have used consistent computational models and modeling assumptions to ensure consistent comparisons of the actual impacts of reactor operating parameters for BWR BUC. All of these studies have considered independent variations of the

operating parameters, and studies of correlated parameters are planned for the next investigative phase.

The assessments documented here were not exhaustive, as they were based on specific assembly and cask configurations and limited BWR plant operating data. Moreover, the calculated cask reactivity effects were determined for a single assembly average burnup (45.2 GWd/MTU) and therefore do not quantify the burnup dependence of these effects. However, the established trends in cask reactivity with independent variations of the considered operating parameters are consistent with findings from other studies [1,12,14].

The directions and magnitudes of impacts on cask reactivity are briefly summarized below for each reactor operating parameter assessed in this work.

Fuel temperature

- Cask reactivity increased linearly with increasing fuel temperature over the range of 596–1296 K for each AO and AFP isotope set.
- The magnitude of the cask reactivity increase was slightly larger for the AO set than for the AFP set (~1.1 pcm/K for AO and ~1.0 pcm/K based on linear fit in Figure 4).
- A bounding value in cask reactivity increase, irrespective of the isotope set used, was 0.12% for every 100 K temperature increase (based on data in Table 2).

Bypass water density

- Cask reactivity increased with decreasing bypass water density for each of the AO and AFP isotope sets.
- The magnitude of the cask reactivity increase was larger for the AO set than for the AFP set (see Figure 5).
- The cask reactivity increase, irrespective of the isotope set used in criticality calculations, was less than 0.1% for every 1% reduction in bypass water density.

Specific power

- Cask reactivity increased with increasing specific power for the AO isotope set, but the magnitude of the increase was very small (~0.02% for 10% specific power increase based on data in Table 4).
- Cask reactivity effect for the AFP isotope set was negligible (based on data in Table 4).

Operating history

- Typical downtimes (~30 days between cycles) have a negligible effect on cask reactivity.
- Extended downtimes preceding an assembly's last irradiation cycle before being discharged led to decreases in cask k_{eff} values. The magnitude of the decreases was similar for the AO and AFP sets given the same power history. Additionally, the magnitude of the decrease varied with the power history.

- Cask reactivity was negligibly affected by the power level during assembly's last irradiation cycle relative to the lifetime-average power.
- Operating history with uniform power levels and no downtime between cycles provided the highest value for cask k_{eff}.

As expected, the results summarized here confirm that the impacts of the operating parameters under consideration are small relative to the impacts of control blade usage, axial moderator density, and axial burnup profile [2,3,12].

Acknowledgments

Funding for this work was provided by the U.S. Nuclear Regulatory Commission (NRC). The authors would like to thank Mourad Aissa and other staff members of the NRC Office of Nuclear Regulatory Research for their helpful comments and support. Special thanks are extended to Steve Bowman, Ian Gauld, and William Marshall from Oak Ridge National Laboratory for reviewing this paper and providing valuable suggestions.

References

1. D. E. Mueller, S. M. Bowman, W. J. Marshall, and J. M. Scaglione, *Review and Prioritization of Technical Issues Related to Burnup Credit for BWR Fuel*, NUREG/CR-7158 (ORNL/TM-2012/261), prepared for the US Nuclear Regulatory Commission by Oak Ridge National Laboratory, Oak Ridge, Tennessee (February 2013).
2. B. J. Ade, W. J. Marshall, S. M. Bowman, and J. S. Martinez, "Effects of Control Blade History, Axial Coolant Density Profiles, and Axial Burnup Profiles on BWR Burnup Credit," *CD Proceedings PHYSOR 2016*, Sun Valley, Idaho (May 2016).
3. W. J. Marshall, B. J. Ade, S. M. Bowman, and J. S. Martinez, *Axial Moderator Density Distributions, Control Blade Usage, and Axial Burnup Distributions for Extended BWR Burnup Credit*, NUREG/CR-7224 (ORNL/TM-2015/544), prepared for the US Nuclear Regulatory Commission by Oak Ridge National Laboratory, Oak Ridge, Tennessee (August 2016).
4. W. J. Marshall, B. J. Ade, S. M. Bowman, I. C. Gauld, G. Ilas, U. Mertyurek, and G. Radulescu, *Technical Basis for Peak Reactivity Burnup Credit for BWR Spent Nuclear Fuel in Storage and Transportation Systems*, NUREG/CR-7194, prepared for the US Nuclear Regulatory Commission by Oak Ridge National Laboratory, Oak Ridge, TN (April 2015).
5. D. E. Mueller, J. M. Scaglione, J. C. Wagner, and S. M. Bowman, *Computational Benchmark for Estimated Reactivity Margin from Fission Products and Minor Actinides in BWR Burnup Credit*, NUREG/CR-7157 (ORNL/TM-2012/96), prepared for the US Nuclear Regulatory Commission by Oak Ridge National Laboratory, Oak Ridge, Tennessee (February 2013).
6. SCALE: *A Comprehensive Modeling and Simulation Suite for Nuclear Safety Analysis and*

Design, ORNL/TM-2005/39, Version 6.1, Oak Ridge National Laboratory, Oak Ridge, Tenn. (June 2011). Available from Radiation Safety Information Computational Center at Oak Ridge National Laboratory as CCC-785.

7. J. C. Wagner, *Computational Benchmark for Estimation of Reactivity Margin from Fission Products and Minor Actinides in PWR Burnup Credit*, NUREG/CR-6747 (ORNL/TM-2000/306), prepared for the US Nuclear Regulatory Commission by Oak Ridge National Laboratory, Oak Ridge, Tennessee (October 2001).
8. M. D. DeHart and S. M. Bowman, "Reactor Physics Methods and Analysis Capabilities in SCALE," *Nuclear Technology*, 174(2), (May 2011): 196–213.
9. I. C. Gauld, G. Radulescu, G. Ilas, B. D. Murphy, M. L. Williams, and D. Wiarda, "Isotopic Depletion and Decay Methods and Analysis Capabilities in SCALE," *Nuclear Technology*, 174(2) (May 2011): 169–195.
10. I. C. Gauld, M. T. Pigni, and G. Ilas, "Validation and Testing of ENDF/B-VII Decay Data," *Nuclear Data Sheets* 120 (2014): 33–36.
11. S. Goluoglu, L. M. Petrie, M. E. Dunn, D. F. Hollenbach, and B. T. Rearden, "Monte Carlo Criticality Methods and Analysis Capabilities in SCALE," *Nuclear Technology*, 174(2) (May 2011): 214–235.
12. J. C. Wagner, M. D. DeHart, and B. L. Broadhead, *Investigation of Burnup Credit Modeling Issues Associated with BWR Fuel*, ORNL/TM-1999/193, Oak Ridge National Laboratory, Oak Ridge, Tennessee (October 2000).
13. D. P. Henderson, *Summary Report of Commercial Reactor Criticality Data for LaSalle Unit 1*, B00000000-01717-5705-00138 REV 00, Civilian Radioactive Waste Management System M&O Contractor (September 1999).
14. C. V. Parks, M. D. DeHart, and J. C. Wagner, *Review and Prioritization of Technical Issues Related to Burnup Credit for LWR*, NUREG/CR-6665 (ORNL/TM-1999/303), prepared for the US Nuclear Regulatory Commission by Oak Ridge National Laboratory, Oak Ridge, Tennessee (February 2000).